Formation elastic parameters and synthetic *P-P* and *P-S* seismograms for the Blackfoot field

Colin C. Potter, Susan L.M. Miller and Gary F. Margrave

ABSTRACT

Formation elastic parameters were calculated from blocked *P*-wave sonic, *S*-wave sonic, and density logs from four wells in the Blackfoot Field. These data and cross plots of well log data from the Glauconitic channel showed a tendency for *Vp/Vs* to increase with shale content. This is primarily due to a decrease in *Vs* with increasing shaliness. Low *Vp/Vs* is a good diagnostic indicator of clean reservoir sand. *P-P* and *P-S* offset synthetic seismograms from these four wells were correlated to the Blackfoot 3C-3D survey at the well locations. Quality of correlation varied between synthetic seismograms and stacked data. There was good overall *P-P* and *P-S* correlation for the 08-08 and 12-16 wells, and the *P-S* correlation was superior to the *P-P* in the 04-16 and 09-17 wells. A different bandpass filter for the 04-16 *P-P* synthetic stack results in better correlation.

INTRODUCTION

A 3C-3D survey was acquired over the Blackfoot-Cavalier Field twenty kilometers south east of Strathmore, Alberta in November, 1995. The purpose of the survey was to use *P-P* and *P-S* seismic data to delineate Glauconitic incised valleys, and to distinguish between sand and shale valley fill. The purpose of the work presented here is to provide formation elastic parameters from well log data. These parameters are made available for reference and for input into further analyses. The well logs were also used to generate *P-P* and *P-S* offset synthetic seismograms, which were then correlated to the *P-P* and *P-S* 3D seismic surveys.

The geology of the Blackfoot Field was discussed by Miller et al. (1995) in Volume 7 of the CREWES Research Report. This is a brief review of the lithology of the formations of interest in this paper. The Glauconitic consists of very fine to medium grained quartz sandstone in the eastern part of Alberta, and glauconite is only common northwards of central Alberta. The sediments of the channel in this study are subdivided into three units corresponding to three phases of valley incision; all three cuts may not be present everywhere. The lower and upper members are made up of quartz sandstones with an average porosity of approximately 18%, while the middle member is a relatively denser lithic sandstone. The channel sands shale out in some locations, such as at the 12-16 well. The primary hydrocarbon is oil, although gas may also be present in the upper member. The individual members range in thickness from 5-20 m.

The incised valley cuts to varying depths through the underlying strata and thus the base may be found directly overlying one of several formations. The Ostracod beds underlying the Glauconitic are made up of brackish water shales, argillaceous, fossiliferous limestones and thin quartz sandstones and siltstones (Layer, D. B. et al, 1949). The Sunburst Member contains ribbon and sheet sandstones made up of sub-litharenites and quartzarenites. The Detrital Beds make up the basal part of the Mannville Group. This unit has an extremely heterogeneous lithology containing chert pebbles, lithic sandstone, siltstone and abundant shale. Its distribution is largely controlled by depressions in the pre-Cretaceous erosional surface and, as such, its thickness is also highly variable over short distances. Within the study area, the

Mannville Group lies unconformably over Mississippian carbonates of the Shunda Formation. The erosional contact surface has an irregular topography and, as the Shunda is shalier up-section, it cuts into varying lithologies.

The elastic rock parameters are useful for characterizing the reservoir, and the elastic-wave synthetic seismograms provide a tie between well log data and seismic data. The following section reviews the relationship between velocity and various rock parameters.

BACKGROUND

Seismic velocities are affected by numerous geologic factors, including rock matrix mineralogy, porosity, pore geometry, pore fluid, bulk density, effective stress, depth of burial, type and degree of cementation, and degree and orientation of fracturing (McCormack et al., 1985). Deciphering the lithologic information inherent in seismic elastic-wave velocities requires an understanding of the relationship between geology and velocity. In order to understand how rock properties influence velocity, researchers have employed a variety of approaches, such as core analysis, well log and seismic interpretation, and numerical modelling (e.g., Kuster and Toksöz, 1974; Gregory, 1977; Eastwood and Castagna, 1983; McCormack et al., 1984). Well log studies are useful because logs provide us with independent measurements of various rock properties of interest. As explorationists, we are particularly interested in formation porosity, permeability, and pore fluid. We also want to identify lithologic variations between reservoir rock and non-reservoir rock. Ultimately, the goal is to deduce petrophysical information from multicomponent seismic data.

To establish correlations between elastic-wave velocities and other rock properties, it is useful to think about how seismic waves propagate. In the case of shear waves, where particle motion is perpendicular to the direction of wave propagation, the rock undergoes a shearing stress which changes its shape, but not its volume. The more that a material resists the shear stress, the greater the shear velocity. In the case of compressional waves, where particle motion is parallel to the direction of wave propagation, the rock undergoes a compressional stress which causes a change in both shape and volume. Again, the more the material resists this deformation, the higher the velocity of the propagating wave. The mode of wave propagation is reflected in the equations for Vp and Vs, where the rigidity modulus (μ) is a measure of the resistance to shearing stress, and the bulk modulus (κ) is a measure of the incompressibility. Both Vp and Vs are inversely related to density (ρ).

$$Vp = \sqrt{\frac{k + \frac{4}{3}\mu}{\rho}} \quad (1) \qquad Vs = \sqrt{\frac{\mu}{\rho}} \quad (2)$$

The equations indicate that if all other factors stay equal, an increase in density will lower both Vp and Vs; however, increases in formation density are usually accompanied by proportionately larger increases in the rigidity and/or incompressibility of the rock. For example, the increase in density which sediments undergo when they are buried, compacted, cemented, and lithified, coincides with a greater increase of the rigidness and incompressibility of the material, so that the seismic velocities increase.

Density is empirically related to porosity by the following equation:

$$\rho_b = \rho_f \phi + \rho_m (1 - \phi) \tag{3}$$

where: ρ_b = bulk density

ρ_f = pore fluid density

ϕ = porosity

ρ_m = matrix density

Vp, *Vs* and bulk density (ρ) can be used to calculate other elastic moduli, including Young's modulus (E), Poisson's ration (σ), rigidity modulus (μ), bulk modulus (κ), Lame's constant (λ). The equations relating these parameters are shown in Table 1 (Sheriff and Geldart, 1995)

Poisson's ratio (σ) is another elastic parameter that can improve predictions about mineralogy, porosity, and reservoir fluid type (e.g. Pickett, 1963; Tatham, 1982; Rafavich et al, 1984; Miller and Stewart, 1990). In a static sense, σ is the ratio of fractional lateral contraction to fractional longitudinal extension when a rod is stretched (Sheriff, 1991). Thus, σ tends to be high in 'soft' materials, and low in stiffer materials. Poisson's ratio can be dynamically related to elastic-wave velocities by the following equations:

$$\sigma = \frac{.5\left(\frac{Vp}{Vs}\right)^2 - 1}{\left(\frac{Vp}{Vs}\right)^2 - 1} \tag{4} \qquad \frac{Vp}{Vs} = \sqrt{\frac{1-\sigma}{.5-\sigma}} \tag{5}$$

Vp/Vs increases monotonically as σ increases. Thus, we expect softer rocks, such as unconsolidated sediments or shales, to have high values of *Vp/Vs*, and hard rocks, such as consolidated clastics and carbonates, to have lower values of *Vp/Vs*.

Velocity and lithology

P-wave velocity alone is not a good lithology indicator because of the overlap in *Vp* for various rock types. The additional information provided by *Vs* can reduce the ambiguity involved in interpretation. Pickett (1963) demonstrated the potential of *Vp/Vs* as a lithology indicator through his laboratory research. Using core measurements he determined *Vp/Vs* values of 1.9 for limestone, 1.8 for dolomite, 1.7 for calcareous sandstone, and 1.6 for clean sandstone. Subsequent research has generally confirmed these values, and has also indicated that *Vp/Vs* in mixed lithologies varies linearly between the limits of *Vp/Vs* for the end members (Nations, 1974; Kithas, 1976; Eastwood and Castagna, 1983; Rafavich et al., 1984; Wilkens et al, 1984; Castagna et al., 1985, Miller and Stewart, 1990).

Clay content is a significant factor in the study of velocity-porosity relationships in clastic silicate rocks. A number of workers have included a clay term in empirical linear regression equations developed from core analysis data (Tosaya and Nur, 1982; Castagna et al., 1985; Han et al., 1986; King et al., 1988; Eberhart-Phillips et al., 1989). When both porosity and clay effects were studied, porosity was shown to be the dominant effect by a factor of about 3 or 4 (Tosaya and Nur, 1982; Han et al., 1986; King et al., 1988). Vernik and Nur (1991) observed that correlations between

velocity and porosity in sandstones improved significantly if sandstones were divided into separate categories based on clay volume.

Clay which is incorporated into the rock matrix, or is layered between more competent rocks, will make the rock less able to resist shearing forces. Lowering the rigidity of the rock lowers both *Vp* and *Vs*, but has a greater affect on *Vs*, resulting in an overall increase in *Vp/Vs* (Minear, 1982). This result has been observed in core studies of clastic silicates (Han et al., 1986; King et al., 1988) and well logging studies of clastic silicates (Castagna et al., 1985). The increase in *Vp/Vs* with shaliness has been used in seismic field studies to outline sandstone channels encased in shales (Garotta et al, 1985; McCormack et al, 1984). Garrotta et al. (1985) used *Vs/Vp* analysis of a 3-C survey to predict sand/shale ratios in a Viking channel in the Winfield Oil Field in Alberta. A increase in *Vs/Vp* correlated with an increase in sand channel thickness as determined from well log data. McCormack et al. (1985) used *Vp/Vs* analysis to identify sandstones encased in shales in the Morrow Formation in the Empire Abo Field of New Mexico. They observed a decrease in *Vp/Vs* moving along the line from a dry hole to a productive well. The effects of porosity, gas saturation, and sand/shale ratios were modelled; the best fit to the data was a model of increasing sandstone content.

Comparison of sonic logs and seismic data

The data presented in this paper are obtained from borehole logs. When using these data to interpret multicomponent seismic data, there are several factors to consider. Well logs sample a thin annulus around the borehole, whereas surface seismic and VSPs sample average rock properties over large areas of unaltered rock. The depth of penetration of acoustic logs is dependent on signal frequency, and transmitter and receiver spacing, but is generally about one sonic wavelength (Paillet and Cheng, 1991).

The rock in the region of the borehole is altered by the drilling process. Fluid invasion, borehole washouts, fractures, and mud cake affect the well log readings. By using longer spacing and lower frequencies, full-waveform tools attempt to penetrate beyond this altered zone. Other factors which influence log measurements include the presence of clay or gas, and tool effects such as tilting.

The frequency of the log signal is tens of kHz, compared to the seismic signal of tens of Hz. Because it has a much shorter wavelength, the sonic log signal may be influenced by small scale features in the travel path, such as mineral inclusions. Fractures and bed boundaries act as discrete discontinuities to the high frequency signal. At the longer wavelength used in surface seismic surveys, all of these features are averaged into the bulk properties of the rock (Liu, 1987; Paillet and Cheng, 1991). Conversely, the seismic wavefield will respond to lateral facies changes and large scale heterogeneities which are not visible at the well bore. In a vertical well, the travel path of the log signal is close to vertical, whereas seismic rays travel at an angle which is dependent on offset and depth. In rocks where layering, fractures, or other features have caused velocity anisotropy, the sonic log data and the seismic data may be recording different quantities. Because of the bandwidth difference, sonic and seismic wave trains have different velocity dispersion characteristics. In the case of normal dispersion, high frequencies travel faster than low frequencies, so that the integrated sonic log travel times are generally shorter than seismic travel times (Stewart et al., 1984).

The *Vp* and *Vs* values presented in this paper were obtained from the *P* and *S* transit times from dipole sonic logs. These tools use a dipole source to generate a flexural wave which deforms the borehole. The first arrival travels at the same velocity as the *S*-wave, and no Stoneley wave is generated. *P* waves are recorded using an alternately firing monopole source. Dipole tools can also be run in cased holes.

FORMATION ELASTIC PARAMETERS

The parameters in Tables 3 - 6 are taken from log data from four wells (08-08; 04-16; 12-16; and 09-17) in the Blackfoot Field located in Township 23, Range 23 West of the 4th Meridian. These wells were selected because they have dipole sonic logs over the zone of interest in addition to a full suite of conventional logs. The parameters were obtained using MATLAB scientific programming environment. Well logs (*P* sonic, *S* sonic and density) were blocked across the lithological units listed in Table 1 using the LOGEDIT algorithm (Margrave and Foltinek, 1995). The mean value between units was used for blocking. Each depth relates to the top of the formation and it's corresponding interval. The slowness values (us/m) were converted to velocity (m/s) for the *P* sonic and *S* sonic logs. The blocked *Vp*, *Vs* and ρ log values were used to calculate *Vp/Vs*, σ, κ, μ, λ and E using the elastic equations in Table 1. References to the conventions are as follows: *Vp* or α for *P*-wave velocity (m/s); *Vs* or β for *S*-wave velocity (m/s); ρ for density (kg/m3); σ for Poisson's ratio; κ for Bulk modulus (pascals); μ for Rigidity modulus (pascals); λ for Lame's constant (pascals); E for Young's modulus (pascals). The sonic curve data from the Ostracod in the 09-17 well were judged unreliable and therefore not included in the analysis.

Table 2 shows the naming conventions used in Figures 3 - 7, Tables 3 - 6, and other chapters in the 1996 CREWES Research Report Volume 8.

Table 1. Relations between elastic constants and velocities (Sheriff and Geldart, 1995)

	Young's modulus, E	Poisson's ratio, σ	Bulk modulus, k	Shear modulus, μ	Lamé constant, λ	P-wave velocity, α	S-wave velocity, β	Velocity ratio, β/α
(E,σ)			$\dfrac{E}{3(1-2\sigma)}$	$\dfrac{E}{2(1+\sigma)}$	$\dfrac{E\sigma}{(1+\sigma)(1-2\sigma)}$	$\left[\dfrac{E(1-\sigma)}{(1+\sigma)(1-2\sigma)\rho}\right]^{1/2}$	$\left[\dfrac{E}{2(1+\sigma)\rho}\right]^{1/2}$	$\left[\dfrac{1-2\sigma}{2(1-\sigma)}\right]^{1/2}$
(E,k)		$\dfrac{3k-E}{6k}$		$\dfrac{3kE}{9k-E}$	$3k\left(\dfrac{3k-E}{9k-E}\right)$	$\left[\dfrac{3k(3k+E)}{\rho(9k-E)}\right]^{1/2}$	$\left[\dfrac{3kE}{(9k-E)\rho}\right]^{1/2}$	$\left(\dfrac{E}{3k+E}\right)^{1/2}$
(E,μ)		$\dfrac{E-2\mu}{2\mu}$	$\dfrac{\mu E}{3(3\mu-E)}$		$\mu\left(\dfrac{E-2\mu}{3\mu-E}\right)$	$\left[\dfrac{\mu(4\mu-E)}{(3\mu-E)\rho}\right]^{1/2}$	$\left(\dfrac{\mu}{\rho}\right)^{1/2}$	$\left(\dfrac{3\mu-E}{4\mu-E}\right)^{1/2}$
(σ,k)	$3k(1-2\sigma)$			$\dfrac{3k}{2}\left(\dfrac{1-2\sigma}{1+\sigma}\right)$	$3k\left(\dfrac{\sigma}{1+\sigma}\right)$	$\left[\dfrac{3k(1-\sigma)}{\rho(1+\sigma)}\right]^{1/2}$	$\left[\dfrac{3k}{2\rho}\left(\dfrac{1-2\sigma}{1+\sigma}\right)\right]^{1/2}$	$\left[\dfrac{1-2\sigma}{2(1-\sigma)}\right]^{1/2}$
(σ,μ)	$2\mu(1+\sigma)$		$\dfrac{2\mu(1+\sigma)}{3(1-2\sigma)}$		$\mu\left(\dfrac{2\sigma}{1-2\sigma}\right)$	$\left[\left(\dfrac{2\mu}{\rho}\right)\left(\dfrac{1-\sigma}{1-2\sigma}\right)\right]^{1/2}$	$\left(\dfrac{\mu}{\rho}\right)^{1/2}$	$\left[\dfrac{1-2\sigma}{2(1-\sigma)}\right]^{1/2}$
(σ,λ)	$\lambda\dfrac{(1+\sigma)(1-2\sigma)}{\sigma}$		$\lambda\left(\dfrac{1+\sigma}{3\sigma}\right)$	$\lambda\left(\dfrac{1-2\sigma}{2\sigma}\right)$		$\left[\left(\dfrac{\lambda}{\rho\sigma}\right)(1-\sigma)\right]^{1/2}$	$\left[\dfrac{\lambda}{\rho}\left(\dfrac{1-2\sigma}{2\sigma}\right)\right]^{1/2}$	$\left[\dfrac{1-2\sigma}{2(1-\sigma)}\right]^{1/2}$
(k,μ)	$\dfrac{9k\mu}{3k+\mu}$	$\dfrac{3k-2\mu}{2(3k+\mu)}$			$k-2\mu/3$	$\left(\dfrac{k+4\mu/3}{\rho}\right)^{1/2}$	$\left(\dfrac{\mu}{\rho}\right)^{1/2}$	$\left(\dfrac{\mu}{k+4\mu/3}\right)^{1/2}$
(k,λ)	$9k\left(\dfrac{k-\lambda}{3k-\lambda}\right)$	$\dfrac{\lambda}{3k-\lambda}$		$\dfrac{3}{2}(k-\lambda)$		$\left(\dfrac{3k-2\lambda}{\rho}\right)^{1/2}$	$\left[\dfrac{3(k-\lambda)}{2\rho}\right]^{1/2}$	$\left[\dfrac{1}{2}\left(\dfrac{k-\lambda}{k-2\lambda/3}\right)\right]^{1/2}$
(μ,λ)	$\mu\left(\dfrac{3\lambda+2\mu}{\lambda+\mu}\right)$	$\dfrac{\lambda}{2(\lambda+\mu)}$	$\lambda+\dfrac{2}{3}\mu$			$\left(\dfrac{\lambda+2\mu}{\rho}\right)^{1/2}$	$\left(\dfrac{\mu}{\rho}\right)^{1/2}$	$\left(\dfrac{\mu}{\lambda+2\mu}\right)^{1/2}$
(α,β)	$\rho\beta^2\left(\dfrac{3\alpha^2-4\beta^2}{\alpha^2-\beta^2}\right)$	$\dfrac{\alpha^2-2\beta^2}{2(\alpha^2-\beta^2)}$	$\rho\left(\alpha^2-\dfrac{4}{3}\beta^2\right)$	$\rho\beta^2$	$\rho(\alpha^2-2\beta^2)$			

Table 2. Formation naming conventions

Abbreviation	Unit Name
2WS	Second White Speckled Shale
BFS	Base of Fish Scales Zone
VIKING	Viking
MANN	Blairmore - Upper Mannville
COAL 1	1st Coal Layer
COAL 2	2nd Coal Layer
COAL 3	3rd Coal Layer
GLCTOP	Glauconitic Channel Top
LITHCH	Lithic Channel Unit
GLCSS	Glauconitic Channel Porous Sandstone Unit
OST	Ostracod
SUNB	Sunburst
DET	Detrital
MISS	Shunda - Mississippian

Table 3. Formation parameters for 08-08 (oil well on channel)

Fm	Depth	Vp	Vs	Vp/Vs	σ	ρ	κ	μ	λ	E
Units	m	m/s	m/s	-	-	kg/m3	e10Pa	e10Pa	e10Pa	e10Pa
above	1362	3872	2030	1.907	0.310	2500	2.374	1.030	1.687	2.700
MANN	1432	3978	2097	1.897	0.307	2512	2.501	1.105	1.765	2.890
COAL 1	1504	3700	2117	1.747	0.256	2366	1.824	1.060	1.117	2.665
COAL 2	1512	3996	2233	1.790	0.273	2437	2.271	1.214	1.461	3.093
COAL 3	1524	4064	2098	1.937	0.318	2495	2.656	1.097	1.924	2.895
GLCTOP	1552	3860	2322	1.662	0.216	2412	1.859	1.300	0.992	3.163
LITHCH	1576	4299	2513	1.710	0.240	2530	2.544	1.598	1.478	3.964
GLCSS	1582	3783	2295	1.648	0.208	2383	1.735	1.255	0.898	3.035
DET	1595	4256	2506	1.698	0.234	2521	2.455	1.583	1.399	3.909
MISS	1612	6008	3116	1.928	0.316	2661	6.160	2.584	4.438	6.801

Table 4. Formation parameters for 04-16 (shale filled channel)

Fm	Depth	Vp	Vs	Vp/Vs	σ	ρ	κ	μ	λ	E
Units	m	m/s	m/s	-	-	kg/m3	e10Pa	e10Pa	e10Pa	e10Pa
above	1180	3475	1815	1.914	0.312	2536	1.948	0.835	1.391	2.193
2WS	1227	3535	1851	1.910	0.311	2535	2.009	0.868	1.430	2.277
BFS	1315	3291	1516	2.171	0.365	2475	1.922	0.568	1.543	1.553
VIKING	1338	3826	1995	1.918	0.313	2513	2.345	0.999	1.679	2.626
MANN	1433	3980	2018	1.972	0.326	2517	2.619	1.025	1.936	2.720
COAL 1	1511	3396	1662	2.044	0.342	2259	1.773	0.623	1.358	1.675
COAL 2	1518	4177	2100	1.989	0.330	2547	2.945	1.122	2.197	2.988
COAL 3	1529	3964	2042	1.941	0.319	2544	2.583	1.061	1.876	2.800
GLCTOP	1561	4053	2110	1.921	0.314	2574	2.700	1.145	1.936	3.011
SUNB	1580	4377	2320	1.887	0.304	2566	3.074	1.380	2.154	3.603
DET	1589	4418	2396	1.844	0.291	2519	2.989	1.446	2.025	3.736
MISS	1625	5477	2870	1.908	0.310	2393	4.549	1.970	3.235	5.167

Table 5. Formation parameters for 12-16 (shale filled channel)

Fm	Depth	Vp	Vs	Vp/Vs	σ	ρ	κ	μ	λ	E
Units	m	m/s	m/s	-	-	kg/m3	e10Pa	e10Pa	e10Pa	e10Pa
above	1229	3562	1837	1.939	0.318	2512	2.057	0.847	1.492	2.236
2WS	1241	3557	1819	1.955	0.322	2485	2.046	0.822	1.498	2.176
BFS	1328	3303	1520	2.173	0.365	2390	1.871	0.552	1.503	1.509
VIKING	1353	3865	2008	1.925	0.315	2516	2.405	1.014	1.729	2.668
MANN	1445	3987	2018	1.975	0.327	2525	2.642	1.028	1.956	2.731
COAL 1	1519	3485	1683	2.071	0.348	2256	1.887	0.638	1.462	1.722
COAL 2	1525	4121	2120	1.944	0.320	2472	2.717	1.111	1.976	2.933
COAL 3	1538	4071	2103	1.936	0.318	2516	2.687	1.112	1.946	2.932
GLCTOP	1566	3999	2113	1.892	0.306	2558	2.567	1.142	1.805	2.985
GLCSS	1586	4062	2297	1.769	0.265	2493	2.359	1.314	1.482	3.327
DET	1595	4458	2339	1.906	0.310	2571	3.234	1.405	2.297	3.684
MISS	1611	5897	3063	1.925	0.315	2690	5.987	2.524	4.304	6.639

Table 6. Formation parameters for 09-17 (regional)

Fm	Depth	V_p	V_s	V_p/V_s	σ	ρ	κ	μ	λ	E
Units	m	m/s	m/s	-	-	kg/m3	e10Pa	e10Pa	e10Pa	e10Pa
above	1440	3597	1865	1.928	0.316	2547	2.113	0.886	1.522	2.333
MANN	1450	3862	2011	1.920	0.314	2528	2.407	1.022	1.725	2.687
COAL 1	1526	3416	1659	2.059	0.345	2305	1.844	0.634	1.420	1.708
COAL 2	1532	3971	1996	1.989	0.330	2508	2.622	0.999	1.956	2.661
COAL 3	1545	3890	2031	1.916	0.312	2561	2.466	1.055	1.762	2.772
SUNB	1593	4072	2122	1.919	0.313	2550	2.696	1.148	1.931	3.017
DET	1606	4170	2184	1.909	0.311	2538	2.798	1.210	1.991	3.174
MISS	1637	5061	2421	2.091	0.351	2669	4.751	1.564	3.708	4.229

Although these data are provided primarily as a reference, we can make several observations directly from the tables. In the 08-08 well, *Vp/Vs* is lowest in the porous upper and lower units (1.66 and 1.65 respectively). The middle lithic unit is somewhat higher (1.71), but still within range for a sandstone. By contrast, *Vp/Vs* for Glauconitic is significantly higher in the shaley channel wells (1.89 to 1.92). The Glauconitic Channel Porous Sandstone unit within the 12-16 well is composed of 3 meters of sandstone and 6 meters of shale and *Vp/Vs* (1.77) is an intermediate value between sandstone and shale.

In formations outside of the channel, the Detrital *Vp/Vs* values reflect the heterogeneity of this unit, ranging from 1.70 to 1.91. Although the logs terminate in the Mississippian, *Vp/Vs* values of 1.91 to 2.09 are reasonable for the shaley carbonate facies of the Shunda Formation. The *Vp/Vs* values of the formations above the Channel are generally over 1.92, suggesting significant shale content. Values of 1.92 to 2.07 in 12-16, 04-16, and 09-17 wells are also reasonable for coals. The coals in 08-08 are much lower, but these beds are very thin and difficult to sample adequately.

The relationship between *Vp/Vs* and sand/shale content is analyzed further in the next section.

Analysis of Glauconitic channel data

The data examined here are *P*-wave and *S*-wave transit times from the 08-08, 12-16 and 04-16 dipole sonic logs from the Glauconitic Formation. This formation is largely sandstone in the 08-08 well and primarily shale, with a 3 m layer of sandstone, within the 12-16 well. The 04-16 well is also primarily shale with a dirty sand lens. Transit times were converted to velocity and the gamma logs from the same zone were used for shale estimates.

Figure 1 is a plot of *Vp/Vs* versus gamma log values for the 08-08, 12-16 and 04-16 wells in the Glauconitic formation. The data are very scattered, although there is a general trend for *Vp/Vs* to increase with increasing gamma log values, which in turn reflect increasing shale content. The majority of the data points from the 08-08 well have API values less than 90 and there is a dense cluster of points with values of less than 40 API. Most points from this well have *Vp/Vs* values ranging from 1.55 to 1.75; values indicative of sandstone lithologies (e.g. Miller and Stewart, 1990; Eberhart-Phillips et al., 1989; Han et al., 1986; Castagna et al., 1985). In contrast, most of the 04-16 and 12-16 data points have gamma ray values above 80 API and have *Vp/Vs* values from 1.80 to greater than 2.0. The exceptions are the data points from the thin

layer of sandstone within the Glauconitic Formation shown with hollow circles. These have low gamma readings, generally less than 40 API, and low *Vp/Vs* values, mostly from 1.60 to 1.70. The data points from the sandstone layer plot in a distinctly different region of the graph than the 12-16 data points from the shale section. These results are in agreement with the work of Han et al, 1986, and Castagna et al., 1985, which shows that *Vp/Vs* will increase as shale content increases.

The cause of the increase in *Vp/Vs* with increasing shale content is illustrated by the graph of *Vs* versus *Vp* shown in Figure 2. Using the *P*-wave velocity alone, sandstone from the 08-08 well cannot be distinguished from shale from the 12-16 and 04-16 wells. However, *S*-wave velocities are significantly greater in the 08-08 sandstone section than the 12-16 and 04-16 shale section. Again, the points from the thin 12-16 sandstone layer also have a relatively higher *S*-wave velocity and tend to plot in the same region as the 08-08 data. This plot indicates that the increase in *Vp/Vs* with increasing shaliness is due to *Vs* decreasing while *Vp* remains relatively constant.
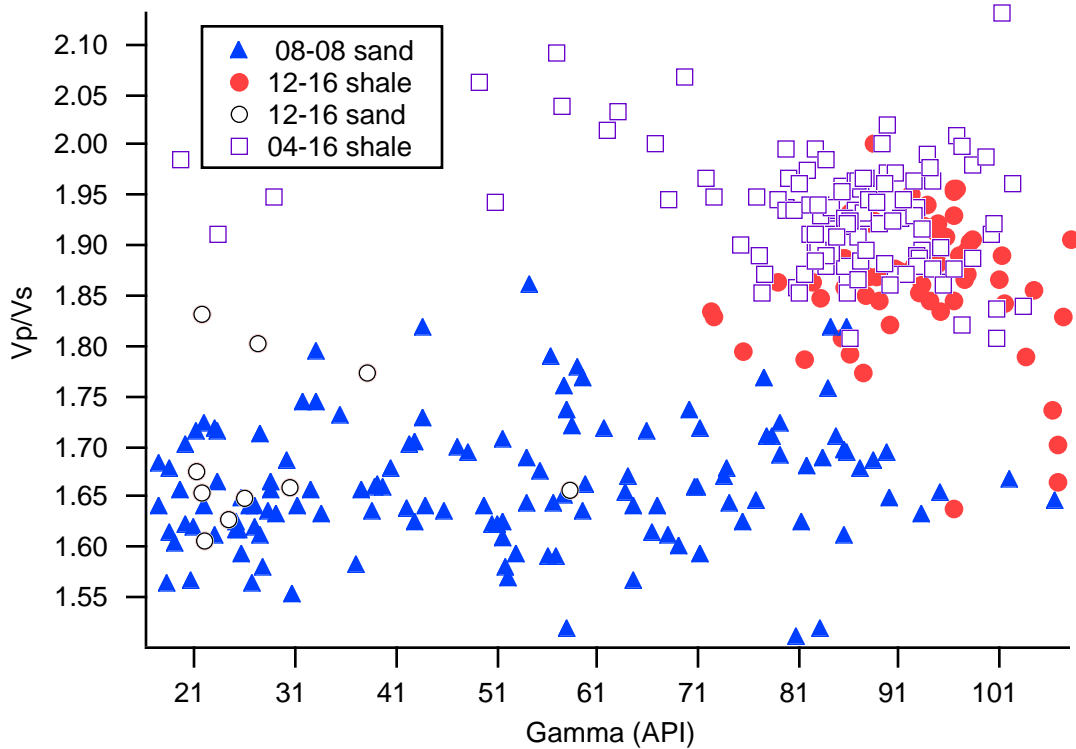
FIG. 1. *Vp/Vs* versus gamma values in the Glauconitic Formation for the 08-08, 04-16 and 12-16 wells.
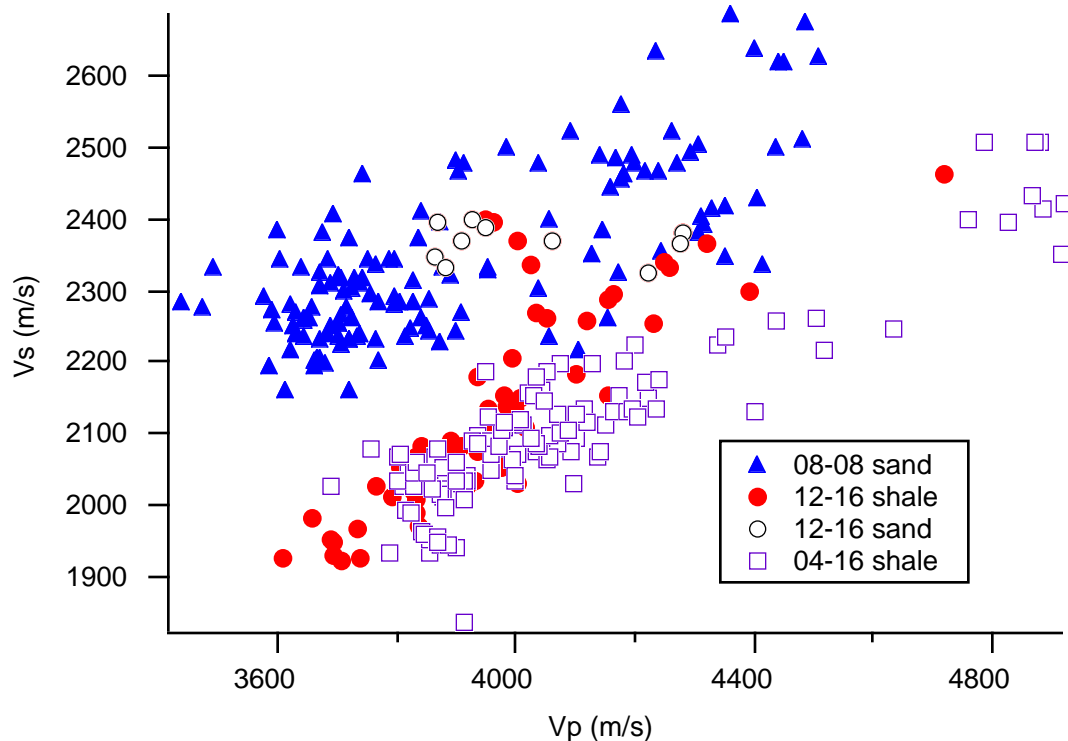
FIG. 2 *Vs* versus *Vp* in the Glauconitic Formation for the 08-08, 04-16 and 12-16 wells.

P-P AND *P-S* SYNTHETIC SEISMOGRAMS

One of the ultimate goals of multicomponent seismic data analysis is to extract rock properties from seismic sections. A critical step in this process is the correlation between synthetic seismograms generated from well logs and seismic data. Figures 3 to 7 show input *P* sonic, *S* sonic and density logs, output *P-P* and *P-S* offset synthetic stacks, and *P-P* and *P-S* seismic data from the Blackfoot 3C-3D survey.

The well logs were sized using the LOGEDIT program in MATLAB. The *P* sonic, *S* sonic and density logs from each well were used for input to the SYNTH program (Lawton and Howell, 1992; Margrave and Foltinek, 1995). The *P-P* and *P-S* offset synthetic seismograms were generated from the SYNTH Algorithm as implemented in MATLAB. The offset seismograms are stacked and four traces are displayed. The synthetic seismograms have not been check shot corrected. The parameters used to generate the offset synthetic stacks are listed below.

PARAMETER	VARIABLES
receiver type	Vertical (*P-P*), horizontal (*P-S*)
near offset	0 m
capture radius	10 m
number of receivers	15
receiver spacing	100 m
offsets	0 to 1500 m
log integration interval	2.0 ms
top layer specifications	*Vp* = 2860 m/s
"	*Vs* = 1430 m/s
"	Density = 2300 kg/m3
synthetic -> reflection type	*P-P*, *P-S*

wavelet (P-P)	10/14-90/100 and 10/14-70/80
wavelet (P-S)	6/10-42/50
sample rate	1 ms
record length	2000 ms

Sensor Geophysical Limited processed the *P-P* and *P-S* seismic data. This data was acquired from Photon's SeisX package point files. These point files consisted of six traces in the inline (E-W) direction at each corresponding well. The third and fourth trace of each data set are closest to each well.

The 08-08 and 09-17 logs extend from above the Blairmore (Mannville) to just below the Shunda (Mississippian). The 12-16 and 04-16 logs extend from above the Second White Speckled Shale to just below the Shunda. Since the logs were all recorded to slightly below the Shunda formation, a full wave cycle below this formation could not be generated for the synthetic seismograms. The synthetic stacks may not be accurate at this formation.
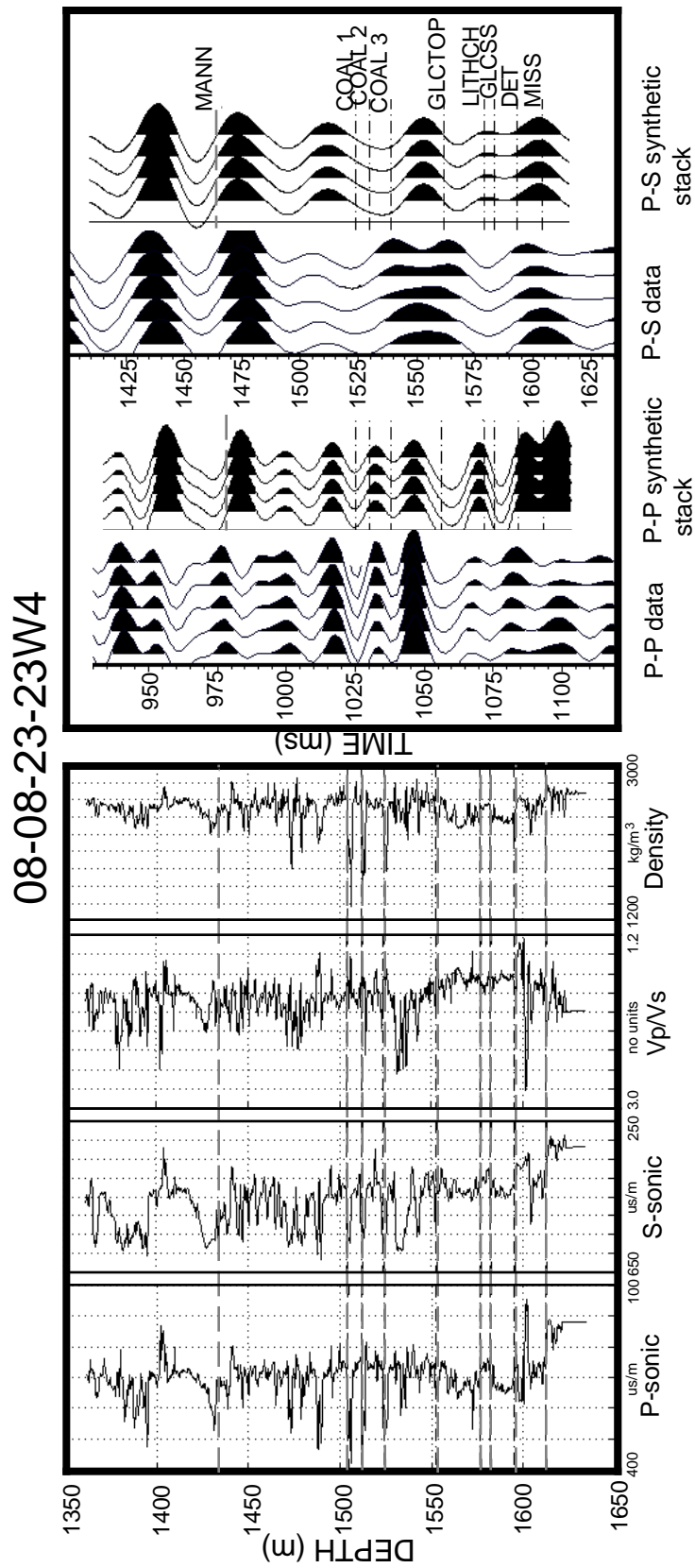
FIG. 3 Correlation of 08-08 well logs in depth with migrated vertical (*P-P* data) and radial (*P-S* data) and the corresponding synthetic stacks in time
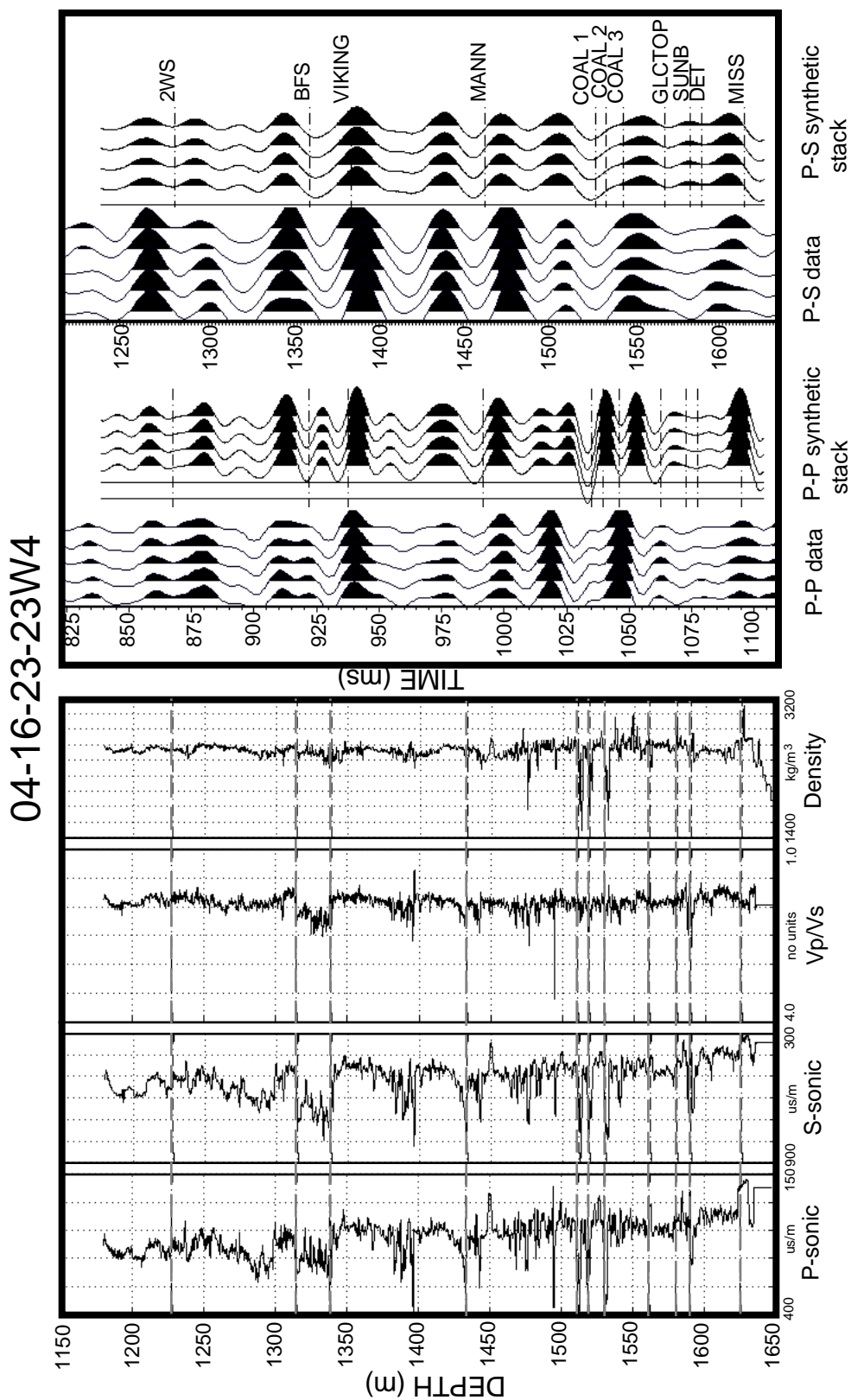
FIG 4. Correlation of 04-16 well logs in depth with migrated vertical (*P-P* data) and radial (*P-S* data) and the corresponding synthetic stacks in time
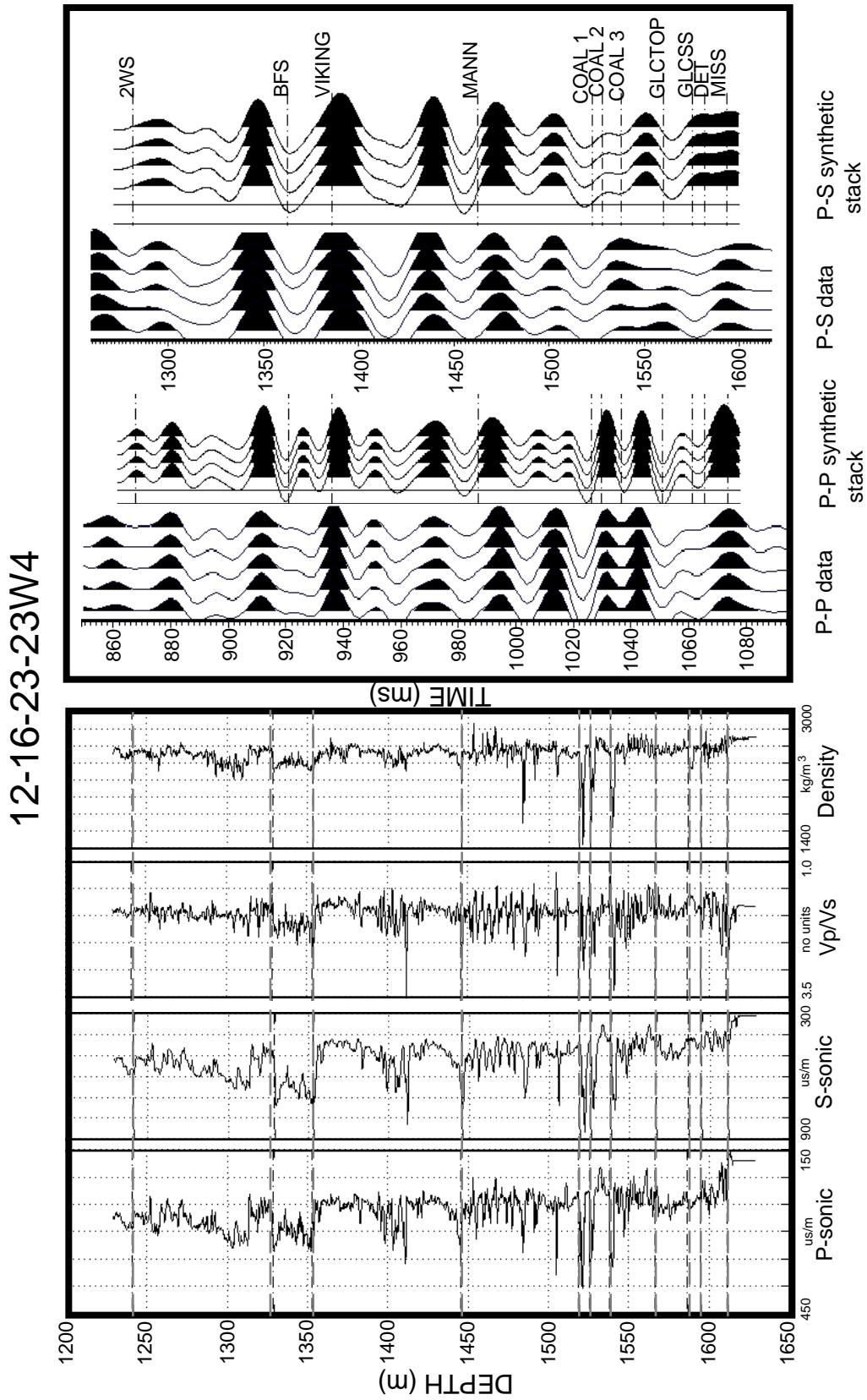
FIG. 5 Correlation of 12-16 well logs in depth with migrated vertical (*P-P* data) and radial (*P-S* data) and the corresponding synthetic stacks in time
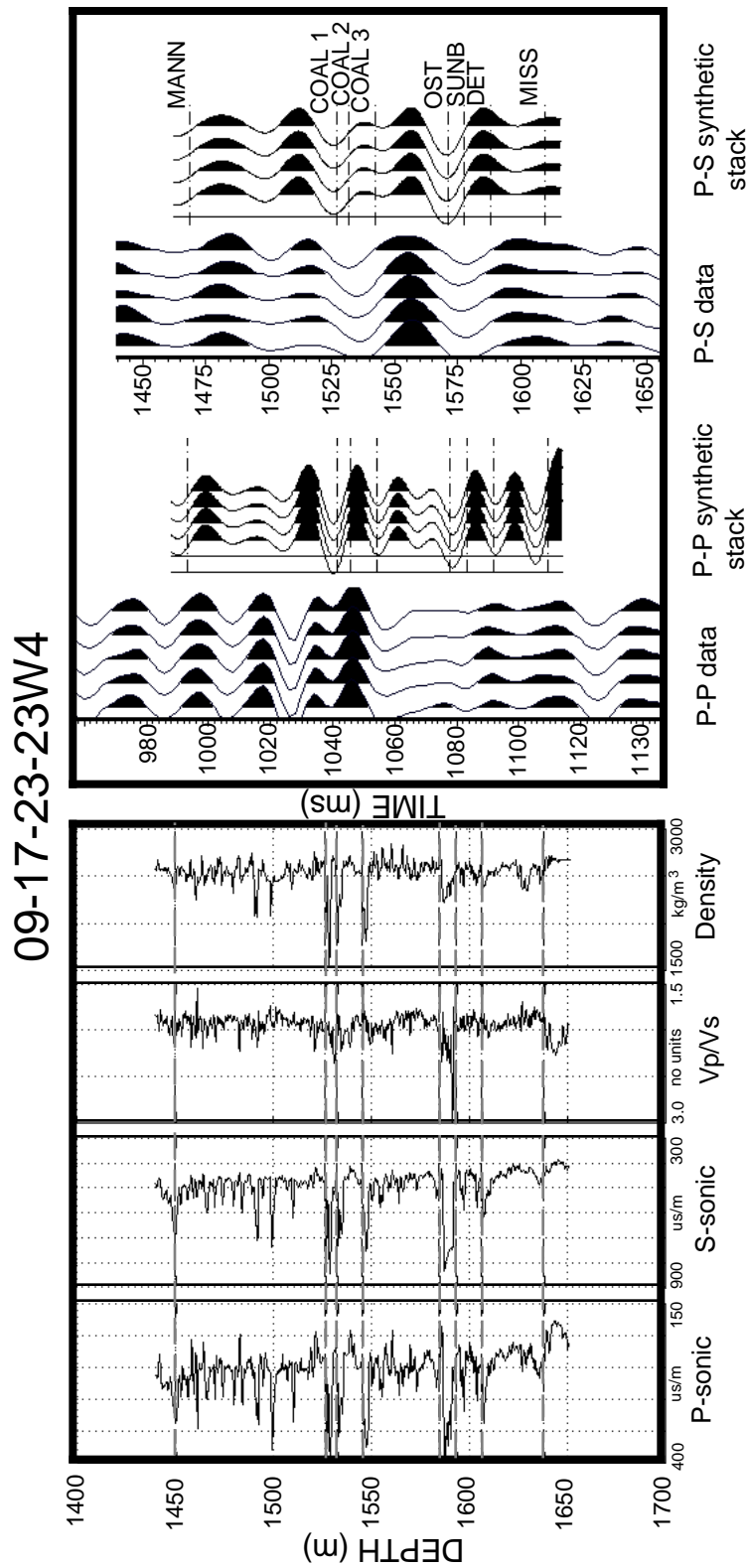
FIG. 6 Correlation of 09-17 well logs in depth with migrated vertical (*P-P* data) and radial (*P-S* data) and the corresponding synthetic stacks in time
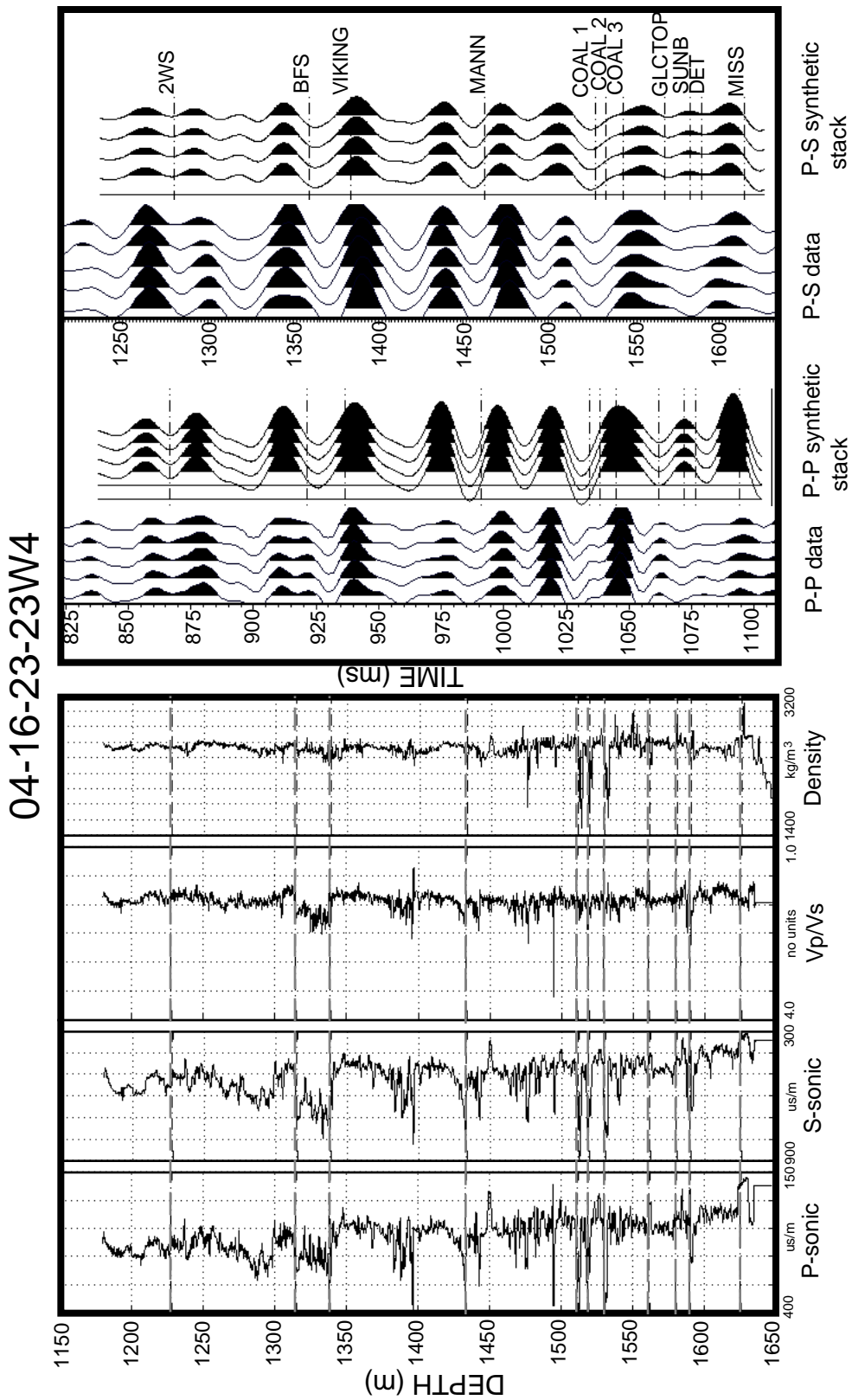
FIG 7. Correlation of 04-16 well logs in depth with migrated vertical (*P-P* data) and radial (*P-S* data) and the corresponding synthetic stacks in time (P-P synthetic stack with 10/14-70/80 filter)

The 08-08 *P-P* and *P-S* data correlation is very good. The *P-P* data and *P-P* synthetic stack correlates well across the coal markers and the channel where the all three units of Glauconitic are observed. The *P-S* correlation is good over all, but the

data is slightly noisy near Glauconitic channel top, probably due to tuning effects. The *P-S* data in 08-08 is changing rapidly across five traces and shows better correlation at trace 2, then between traces 3 and 4 which is at the well location. The 04-16 *P-S* data correlates very well with the *P-S* synthetic stack. The amplitude peak of the Sunburst formation on the *P-S* data does not exist, although in traces 4 and 5 there is indication of a peak forming. The 04-16 *P-P* correlation is reasonable down to 1010 ms, but is poor below this. Figure 7 has much better correlation for the 04-16 *P-P* data than in Figure 4. The *P-P* synthetic stack (Figure 7) was generated with a 10/14-70/80 bandpass filter. The 12-16 *P-P* and *P-S* data correlates very well with the synthetic stacks, except for the *P-P* correlation below 1010 ms. The *P-S* correlation at the channel is excellent down to Coal 1, but deteriorates in the channel where the data becomes noisy. The 09-17 *P-P* data correlates poorly with the synthetic stack, even when a 10/14-70/80 bandpass filter was applied. Conversely, the *P-S* synthetic seismogram ties the data much better.

Generally, the *P-S* correlation is much better than the *P-P* correlation in all the wells. The bandpass filter of 10/14-90/100 used for the *P-P* synthetic seismogram may be too high for the high cut pass. Check shots implementation could result in better correlation.

CONCLUSIONS

Vp/Vs values were calculated from *P* sonic and *S* sonic curves. *Vp/Vs* tends to increase as shale content increases. Low *Vp/Vs* values are a diagnostic indicator of clean sandstones. *Vs* is higher in sandstone than shale while *Vp* is less sensitive, resulting in an overall decrease in *Vp/Vs*. The correlation of the *P* sonic, *S* sonic, *Vp/Vs*, and density logs, synthetic stacked seismograms and the stacked migrated data vary. There was good overall *P-P* and *P-S* correlation in the 08-08 and 12-16 data. For the 04-16 and 09-17 data, *P-S* correlation is superior to *P-P* when using a bandpass filter of 10/14-90/100. A band pass filter of 10/14-70/80 for the 04-16 *P-P* synthetic stack resulted in very good correlation.

FUTURE WORK

Further analysis of formation elastic parameters for all the wells in the Blackfoot Field would improve diagnostics with geostatistical software. *S* sonic logs for all wells could be generated from *P* sonic curves using *Vp/Vs* relationships observed in the formation elastic parameters given here. Then *P-S* seismograms could be generated and correlated all wells to all migrated data sets. Better wavelet extraction is needed to generate specific synthetic seismograms.

ACKNOWLEDGMENTS

REFERENCES

Castagna, J.P., Batzle, M.L., and Eastwood, R.L., 1985, Relationships between compressional-wave and shear-wave velocities in clastic silicate rocks: Geophysics, 50, 571-581.

Eastwood, R.L. and Castagna, J.P., 1983, Basis for interpretation of Vp/Vs ratios in complex lithologies: Soc. Prof. Well Log Analysts 24th Annual Logging Symp.

Eberhart-Phillips, D., Han, D.H., and Zoback, M.D., 1989, Empirical relationships among seismic velocity, effective pressure, porosity, and clay content in sandstone: Geophysics, 54, 82-89.

Garotta, R., Marechal, P., and Megesan, M., 1985, Two-component acquisition as a routine procedure for recording P-waves and converted waves: Journal of the Canadian Society of Exploration Geophysicists, 21, 40-53.

Gregory, A.R., 1977, Aspects of rock physics from laboratory and log data that are important to seismic interpretation, *in* Seismic Stratigraphy - Applications to Hydrocarbon Exploration: AAPG Memoir 26, 15-45.

Han, D.H., Nur, A., and Morgan, D., 1986, Effects of porosity and clay content on wave velocities in sandstones: Geophysics, 51, 2093-2107.

King, M.S., Stauffer, M.R., Yang, H.J.P., and Hajnal, Z., 1988, Elastic-wave and related properties of clastic rocks from the Athabasca Basin, Western Canada: Can. J. Expl. Geophys., 24,110-116.

Kithas, B.A., 1976, Lithology, gas detection, and rock properties from acoustic logging systems: Soc. Prof. Well Log Analysts 17th Annual Symp.

Kuster, G.T. and Toksöz, M.N., 1974, Velocity and attenuation of seismic waves in two-phase media: Part 1. Theoretical formulations: Geophysics, 39, 587-606.

Lawton, D.C., and Howell, T.C., 1992, P-P and P-SV synthetic stacks, Expanded Abstract, 62nd SEG Annual International Meeting, October 25-29, New Orleans, USA, 1344-1347

Layer, D.B. and Members of Staff, Imperial Oil Ltd., 1949, Leduc oil field, Alberta, a Devonian coral reef discovery: Bulletin of the American Association of Petroleum Geologists, 33, 575-602.

Liu, O.Y., 1987, The sources of errors in slowness measurements and an evaluation of full waveform compensation techniques: Soc. Petr. Eng. 62nd Annual Tech. Conf. & Exhib.

McCormack, M.D., Dunbar, J.A. and Sharp, W.W., 1984, A case study of stratigraphic interpretation using shear and compressional seismic data: Geophysics, 49, 509-520.

McCormack, M.D., Dunbar, J.A. and Sharp, W.W., 1985, A stratigraphic interpretation of shear and compressional wave seismic data for the Pennsylvanian Morrow formation of southeastern New Mexico, *in* Seismic Stratigraphy II: AAPG Memoir 39, 225-239.

Margrave, G.F., Foltinek, D.S., 1995, P-P and P-SV cross sections: CREWES Research Report 1995, Ch 5.

Miller, S.L.M., Aydemir, E.Ö. and Margrave, G.F., 1995, Preliminary interpretation of P-P and P-S seismic data from the Blackfoot broad-band survey: CREWES Research Report 1995, Ch 42.

Miller, S.L.M. and Stewart, R.R., 1990, Effects of lithology, porosity and shaliness on P- and S-wave velocities from sonic logs: Can. J. Expl. Geophys., 26, 94-103.

Minear, J.W., 1982, Clay models and acoustic velocities: Soc. Petr. Eng. of AIME 57th Annual Tech. Conf. & Exhib.

Nations, J.F., 1974, Lithology and porosity from acoustic shear and compressional wave transit time relationships: Soc. Prof. Well Log Analysts 15th Annual Symp.

Paillet, F.L. and Cheng, C.H., 1991, Acoustic waves in boreholes: CRC Press, Inc.

Pickett, G.R., 1963, Acoustic character logs and their applications in formation evaluation: J. Petr.Tech., June, 659-667.

Rafavich, F., Kendall, C.H.St.C., and Todd, T.P., 1984, The relationship between acoustic properties and the petrographic character of carbonate rocks: Geophysics, 49, 1622-1636.

Sheriff, R.E., 1991, Encyclopedic Dictionary of Exploration Geophysics, Third Ed., SEG

Sheriff, R.E., and Geldart, L.P., 1995, Exploration Seismology, Cambridge University Press, New York, NY

Stewart, R.R., Huddleston, P.D., and Kan, T.K., 1984, Seismic versus sonic velocities: A vertical seismic profiling study: Geophysics, 49, 1153-1168.

Tatham, R.H., 1982, Vp/Vs and lithology: Geophysics, 47, 336-344.

Tosaya, C. and Nur, A., 1982, Effects of diagenesis and clays on compressional velocities in rocks: Geophys. Res. Lett., 84, 3532-3536.

Vernik, L. and Nur, A., 1991, Lithology prediction in clastic sedimentary rocks using seismic velocities: presented at the 1991 SEG Summer Research Workshop, St. Louis, Missouri.

Wilkens, R., Simmons, G., and Caruso, L., 1984, The ratio Vp/Vs as a discriminant of composition for siliceous limestones: Geophysics, 49, 1850-1860.